1997

NASA/ASEE SUMMER FACULTY FELLOWSHIP PROGRAM

MARSHALL SPACE FLIGHT CENTER
THE UNIVERSITY OF ALABAMA IN HUNTSVILLE

CURRENT AND FUTURE CRITICAL ISSUES IN ROCKET PROPULSION SYSTEMS

Prepared by:	Homayun K. Navaz	Jeff C. Dix
Academic Rank:	Assistant Professor	Student
Institution and Department:	GMI Engineering & Management Institute Department of Mechanical Engineering	

NASA/MSFC:

Office:	Combustion Physics Laboratory
Division:	Engine Systems
MSFC Colleagues:	Klaus W. Gross

INTRODUCTION

The objective of this research was to tackle several problems that are currently of great importance to NASA. In a liquid rocket engine several complex processes take place that are not thoroughly understood. Droplet evaporation, turbulence, finite rate chemistry, instability, and injection/atomization phenomena are some of the critical issues being encountered in a liquid rocket engine environment. Pulse Detonation Engines (PDE) performance, combustion chamber instability analysis, 60K motor flowfield pattern from hydrocarbon fuel combustion, and 3D flowfield analysis for the Combined Cycle engine were of special interest to NASA. During the summer of 1997, we made an attempt to generate computational results for all of the above problems and shed some light on understanding some of the complex physical phenomena. For this purpose, the Liquid Thrust Chamber Performance (LTCP) code (Navaz, et al. 1994), mainly designed for liquid rocket engine applications, was utilized. The following test cases were considered:

1. Characterization of a detonation wave in a Pulse Detonation Tube.
2. 60K Motor wall temperature studies.
3. Propagation of a pressure pulse in a combustion chamber (under single and two-phase flow conditions)
4. Transonic region flowfield analysis affected by viscous effects
5. Exploring the viscous differences between a smooth and a corrugated wall
6. 3D thrust chamber flowfield analysis of the Combined Cycle engine.

CFD ANALYSIS

1. Pulse Detonation Tube

Over the last few years, the pulse detonation engines (PDE) have received a considerable amount of attention, due to their high specific impulse and reduced specific fuel consumption (SFC). These engines can potentially offer high performance due to the rapid detonation process. In this test case, a 2-inch diameter, 6-feet long tube is filled with premixed hydrogen and oxygen at stoichiometric mixture ratio initially at atmospheric pressure, closed at the left and subject to atmospheric back pressure from the right. Slip wall conditions are assumed on the tube wall to simulate a one dimensional flow. The analytical solution of this test case showed a good agreement with the experimental data (Navaz, et al, 1997).

Figure (1a) shows the variation of pressure along the centerline in time. The pressure distribution within the detonation tube has a characteristic form. The reaction process is initiated on the left wall by raising the temperature to 5400 °R for one iteration, i.e., a temperature impulse is imposed momentarily. The resulting detonation wave travels toward the open end while a low pressure wake is formed behind the peak pressure that does not move at the same speed. As a result, the region being at the peak pressure expands in size, therefore, prolonging the time that power can be extracted from the detonation pressure. The blow-down process starts when the detonation front reaches the

open end where a backward traveling wave is also initiated. This wave combines with the still incoming pressure wave and forms a rather complex wave form traveling in both directions. A few milliseconds after the blow-down the pressure decreases and asymptotically reaches the atmospheric pressure.

The pressure history on the closed end wall is shown in Figure (1b). The pressure during the detonation and part of the blow down processes on the closed end wall remains constant. However, when the backward traveling wave initiated at the open end reaches the closed end, the pressure decreases. The pressure at the closed end drops to less than one atmosphere, thereafter, and a pressure oscillation in the tube develops which will eventually decay due to viscous effects.

Several test cases were run varying the oxidizer/fuel (O/F) ratio and the temperature impulse for ignition. By changing the O/F ratio, the value of the peak pressure changed, however, the basic characteristics of the detonation wave remained unchanged. An animation video tape has been generated for this test case and our NASA colleague Mr. Klaus W. Gross can be contacted to provide further information. Figures (2) demonstrate the pressure contours in the tube and the pressure along the centerline at several time intervals during the calculations.

2. 60K FASTRAC Motor Wall Temperature Studies

NASA/MSFC is performing some tests to support the design of the 60K motor. This engine uses liquid RP-1 as fuel and liquid oxygen (LOX) as oxidizer. RP-1 is mostly composed of $C_{12}H_{26}$ which is a rather heavy hydrocarbon. The oxidization process for RP-1 is very complex and can easily involve more than 100 species and 1000 reactions and the formation of soot. Reactions producing soot are numerically stiff and may cause numerical instability. The LTCP code is very robust in treating problems with stiff chemistry. Four different cases were considered for this analysis:

a. 60K motor with RP-1/LOX reaction products being at equilibrium conditions with a mixture ratio of 2.34 and temperature of 6391 °R, uniformly distributed at the injector face. This analysis was performed with 8 species finite rate reactions and an adiabatic wall to calculate the maximum possible temperature on the wall. This test case is referred to as the **One-Zone** 60K motor test case.

b. 60K motor with RP-1/LOX reaction products being at equilibrium conditions at two different mixture ratios; 2.64 for the core flow with a temperature of 6520 °R, and 1.12 for the near wall region at 12.6% of the total mass flow rate with a temperature of 2983 °R. The analysis was performed with 8 species finite rate reactions and adiabatic wall conditions. This test case is referred to as the **Two-Zone** 60K motor test case.

c. 60K motor with RP-1/LOX reaction products being at equilibrium conditions with a mixture ratio of 2.64 uniformly distributed at the injector face except the near wall

region where pure RP-1 is injected in the gaseous phase at 6.67 lbm/s. This test case was performed with 22 species and a mechanism for soot formation. The geometry was similar to the one used in the TDK program, i.e., shorter chamber with two cylindrical arcs connected at throat region with no straight section in between as is the case in the real geometry. This test case is referred to as **TDK-Like Geometry**.

d. This test case is similar to the part (c) except that the real geometry of the 60K motor is ported into the LTCP code. This geometry contains a straight cylindrical section connecting the two arcs at the throat region and slightly elongated combustion chamber. This test case is referred to as **Real Geometry**.

The temperature contours and wall temperature for all of the 60K motor test case are shown in Figures (3). The two-zone test case with 12.6% mass flow rate near the wall region shows the lowest temperature achieved along the wall. Figures (4a) and (4b) show the soot mass fraction contours for test cases (c) and (d). It can be seen that slightly less soot is formed in test case (d). This can be attributed to the fact that some of the soot being formed may have enough time in the chamber to react with residues of oxygen to form carbon oxides.

3. Propagation of a Pressure Pulse in a Combustion Chamber

This test case was selected to study a pressure wave propagation in a combustion chamber. In practice, an artificial explosion is initiated in a combustion chamber, and the pressure wave propagation is monitored. This particular study is oriented toward future instability analysis to mark the threshold of an engine mechanical break down. The following test cases were selected for gaseous and two phase flows:

a. The subsonic and transonic portion of a combustion chamber is operating at steady state in gaseous phase for LOX/RP-1. The total pressure of the chamber is 630 psia. At this time a pressure pulse of 12000 psia at the injector face centerline is introduced for one iteration to simulate an explosion. The pressure wave starts to propagate and reflect. Figures (5) shows a series of snap shots from the pressure contours, pressure across the injector face, at the throat, along the centerline, and along the wall. After the explosion, the high pressure wave front generates a wake behind it that will invoke in a secondary wave originating from the location of explosion. This wave follows the first one and collides with the reflected one from the wall. In this case the pressure wave interacts with the finite rate chemistry calculations. It can be seen that the pressure and subsequently the mass flow rate will change significantly as the pressure disturbance passes through the throat.

b. The subsonic and transonic portion of a combustion chamber is running at steady state in two phase flow mode. H_2/O_2 in gaseous form at mixture ratio of 2 is mixed with 60 μm-diameter oxygen droplets. The droplet number density is assumed to be 10^7droplets/cc. This mixture is uniformly injected to the combustion chamber and burned. At this point, a 12000 psia pressure pulse is momentarily introduced at the

centerline. Figures (6) show the pressure pulse development contours and pressure distribution at the injector face, throat, along the centerline, and along the wall. We have considered hydrogen instead of RP-1 for this test case to simplify the chemistry and also reduce the computer run time . However, we can still observe that the pattern of the pressure wave is quite different from the gaseous flow in part (a) above. The existence of droplets has a damping effect on the pressure wave and reduces the strength of this wave considerably. Figures (7) show the oxygen mass fraction during this disturbance and comparing with the undisturbed state, it can be seen that the evaporation rate of the oxygen droplets will change as they come into contact with the pressure wave front. In this case the atomization process is not affected but the evaporation of the droplets and the finite rate chemistry are coupled with the pressure wave propagation.

An animation video tape of this test case can be requested from our NASA/MSFC colleague Mr. Klaus W. Gross.

4. Transonic Region Flowfield Analysis for the Extent of Viscous Effects

The purpose of this test case was to specify the validity of inviscid or Euler solvers in the throat region of a nozzle. Series of runs were made for small throat radii and varying chamber pressures. It was found that for low chamber pressures the viscous layer becomes thicker in the throat region. If the throat radius is of the same order of magnitude as the viscous layer thickness, any solution with an inviscid code will not be valid. Therefore, a CFD analysis must be performed for small throat engines to observe the extent of the viscous layer, before any Euler equation solution is acceptable.

5. Smooth Versus Corrugated Nozzle Wall

It has been speculated that for nozzle walls with corrugation in flow direction the trapped fluid in the gaps of the wall may act like a buffer between the core flow and the wall surface, thus, reducing the viscous effects and losses associated with such a phenomenon. The LTCP-3D code was employed to conduct this study. A typical corrugated wall is shown in Figure (8a). To simplify the geometry for our study, the geometry was assumed to have two planes of symmetry, one on the top of the circular arc and a second one between the two arcs. Figure (8b) shows the geometry for our computational studies. Four test cases were considered by varying the curvature of the arc from quarter of a circle to a flat plate as shown in Figure (8b).

6. 3D Flowfield Analysis of the Rocket Thrust Chamber in a Combined Cycle (CC) Engine

For this test case LTCP-3D with finite rate chemistry was used to evaluate the performance of the thrust chamber. The combustion chamber of this engine is axisymmetric but the nozzle requires a 3D analysis. The 3D effect in the nozzle is fairly significant such that a coarse grid in circumferencial direction will produce numerical

instability. The analysis was performed on a 65x23x71 grid. This number of grid points is not sufficient enough to resolve the boundary layer, but it is adequate for a first order estimate. Furthermore, our goal was to demonstrate the capability of the LTCP-3D in solving complex 3D flowfield equations with near equilibrium (stiff) finite rate chemistry. Figures (9a) through (9c) exhibit the Mach number contours. A fairly coarse grid in the radial direction was used for this case which made the subsonic viscous layer rather thick causing the information to travel backward from the nozzle to the combustion chamber. Therefore, for a coarse grid some 3D effects in the combustion chamber can be expected. Figures (9d) through (9f) shows the water, H_2, and O_2 mass fractions, respectively. A computer run is being made with a finer mesh to evaluate the specific impulse of the thrust chamber for this engine.

CONCLUSION

During the ten week time period of the Summer Faculty Fellowship Program (SFFP) a variety of important topics were addressed. Some of them were completed, others were started and brought to a state to effectively continue further analysis. It was shown that the LTCP-2D and LTCP-3D codes are capable of solving complex and stiff conservation equations for gaseous and droplet phases in a very robust and efficient manner. These codes can be run on a workstation and personal computers (PC's). Further studies in the area of pulse detonation are necessary to understand the effects of the mixture ratio on the detonation wave characteristics. Furthermore, the conditions at which a Chapman-Jouget detonation wave is initiated should be marked. In combustion chamber instability analysis, the effects of a pressure pulse on the atomization process should be studied. The shear stress analysis for the corrugated walls should be further followed, and last but not least, a 3D analysis for the combustion chamber of the combined cycle engine on a fine mesh is necessary to properly estimate the performance characteristics of this engine.

ACKNOWLEDEMENT

The authors wish to thank NASA/MSFC for their support of the Summer Faculty Fellowship Program (SFFP) and University of Alabama in Huntsville for coordinating the program. The research performed during the summer of 1997, will provide NASA with some guidelines in the design process and is mutually beneficial to us. It is intended to incorporate the above topics in a new Modern Compressible Flow course that is going to be offered at GMI Engineering & Management Institute during the Spring 1998 term.

REFERENCES

Navaz, H. K., and A. D. Dang, Engineering and Numerical Analysis/Users' Guide to the Liquid Thrust Chamber Performance (LTCP) Program, Prepared for NASA/MSFC, Contract No. NAS8-38798, January 1994.

Navaz, H. K. and R. M. Berg, "A Solution to Multi-Phase Flow Equations with Chemistry and Stiff Source Terms for Liquid Rocket Engines," Submitted *to J. of Propulsion and Power*, Aug., 1997.

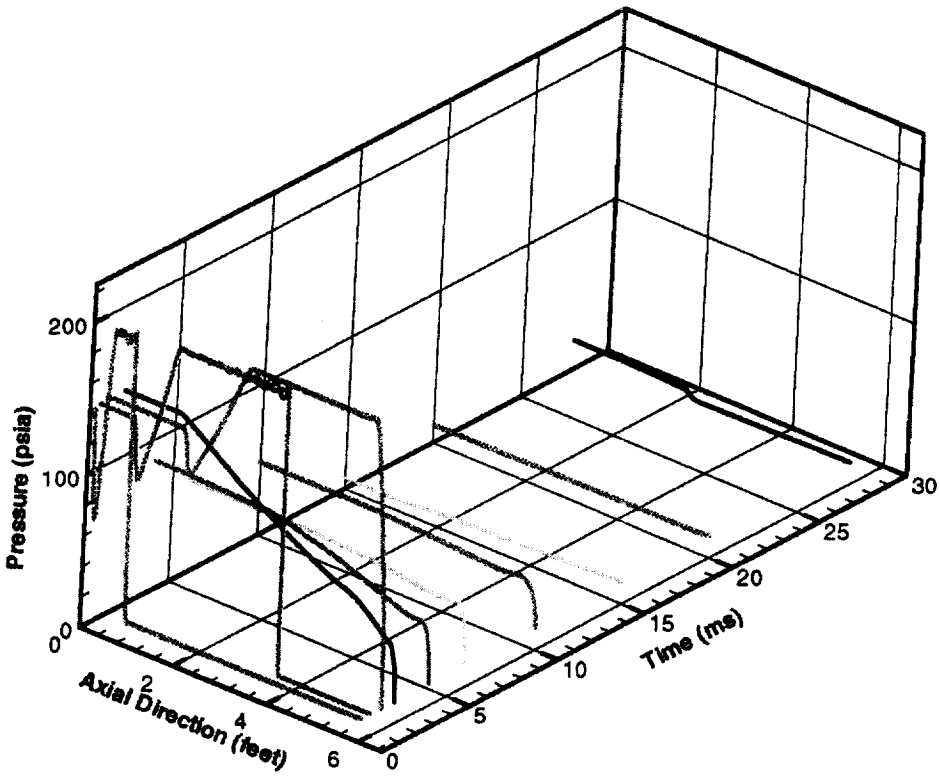

Figure 1a: Pressure history along the tube centerline as a function of time.

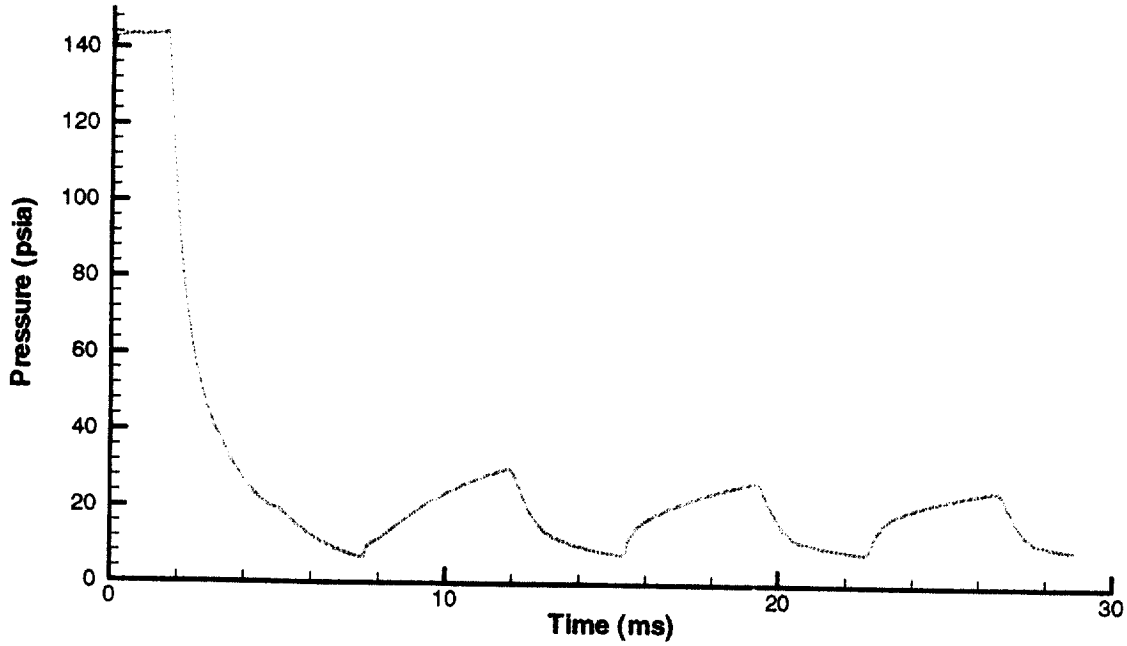

Figure 1b: Pressure history at the closed end of the tube.

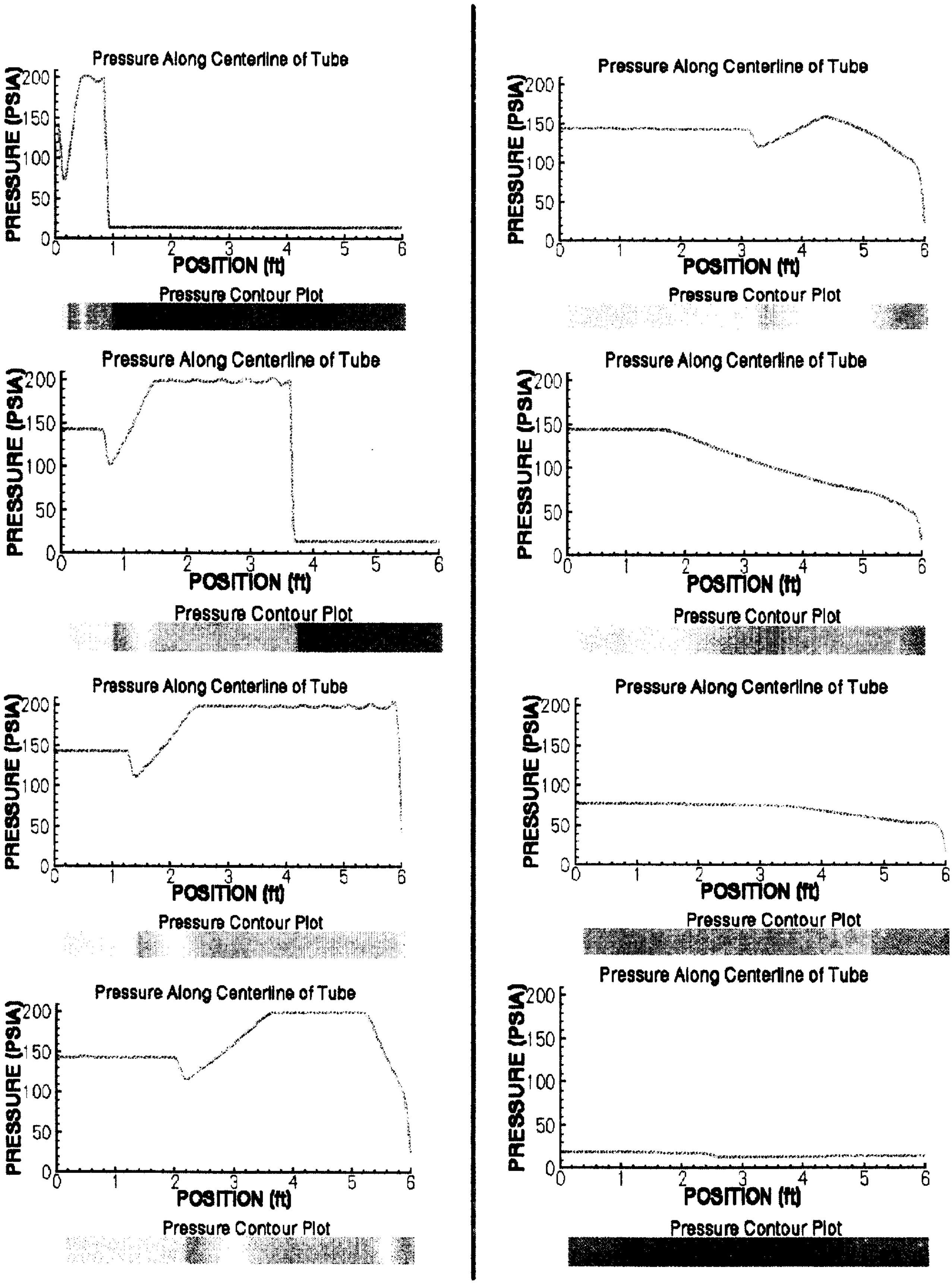

Figure 2: Detonation wave contour and pressure along centerline at several time intervals

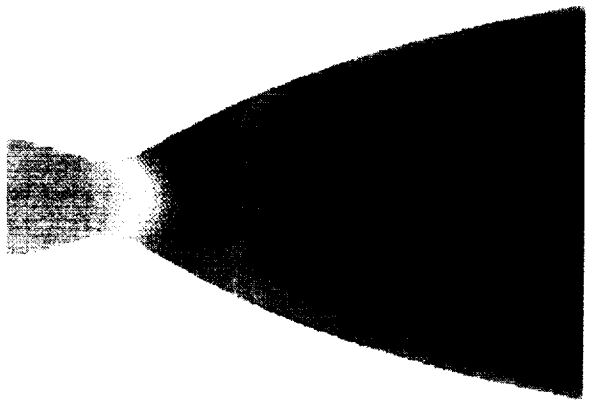

Figure 3a Temperature contours Case (a)

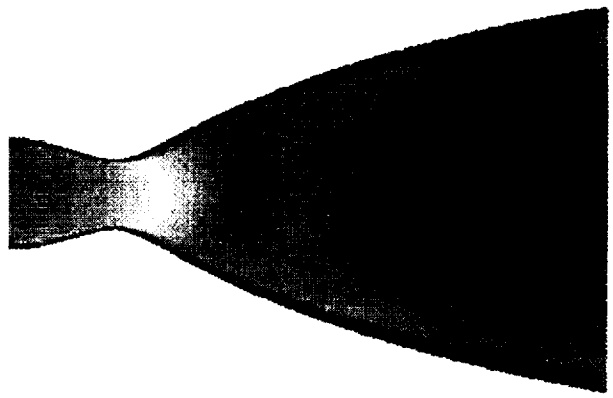

Figure 3b Temperature contours Case (b)

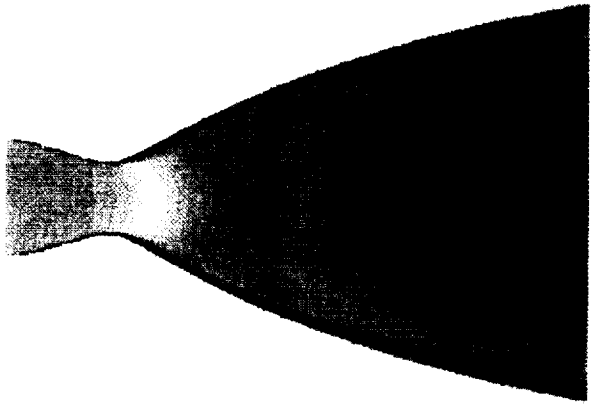

Figure 3c Temperature contours Case (c)

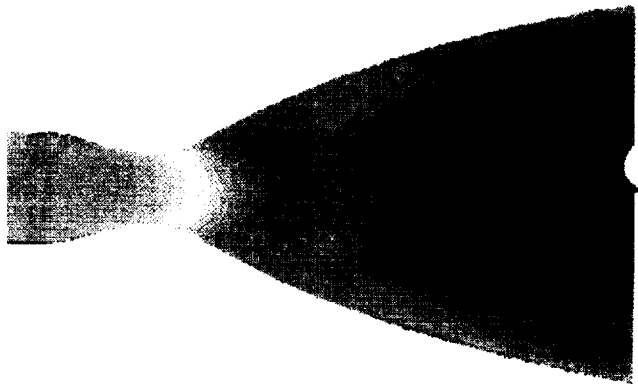

Figure 3d Temperature contours Case (d)

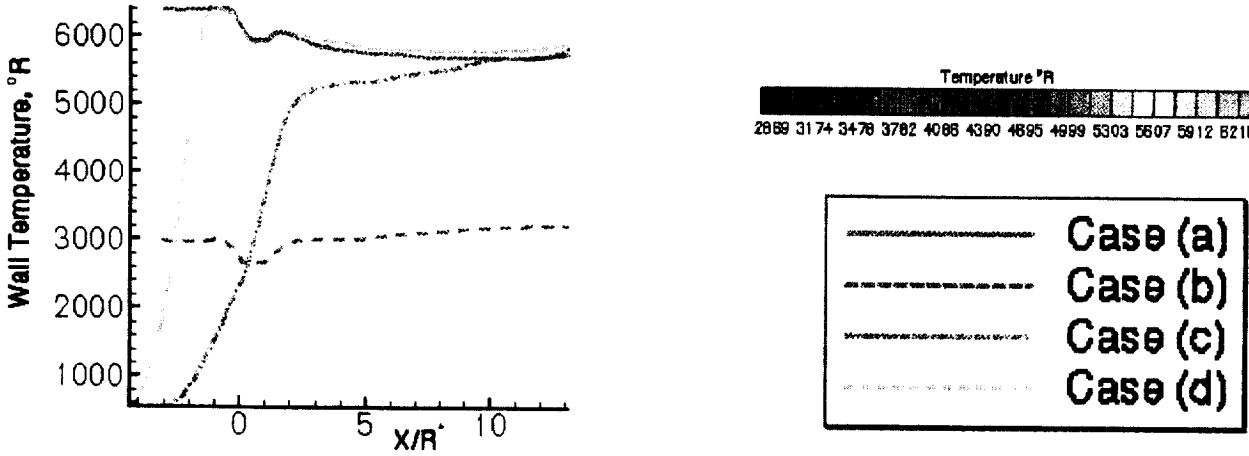

Figure 3e Temperature along the nozzle wall

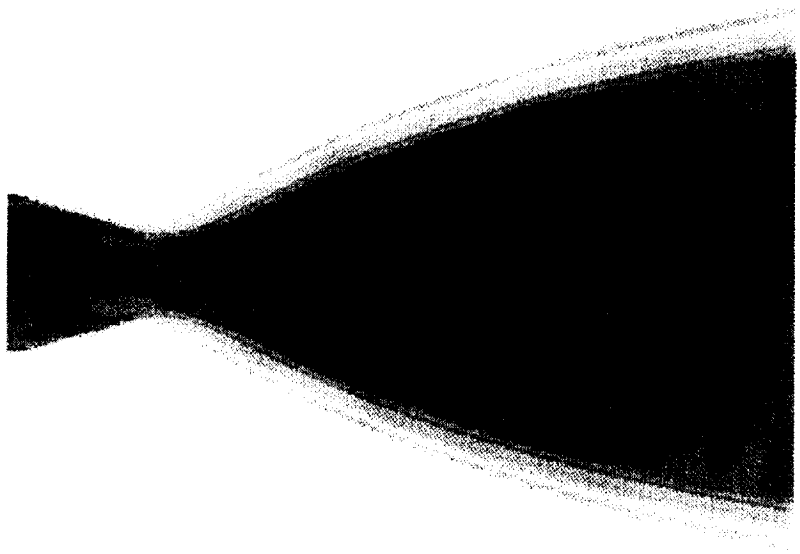

Figure 4a: Mass fraction contours of soot for Case (c).

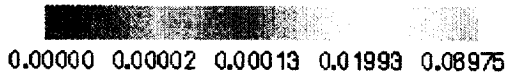

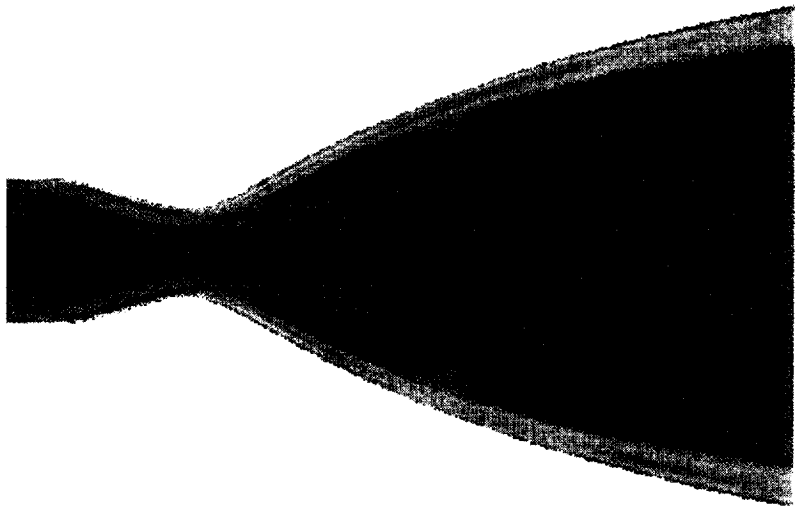

Figure 4b: Mass fraction contours of soot for Case (d).

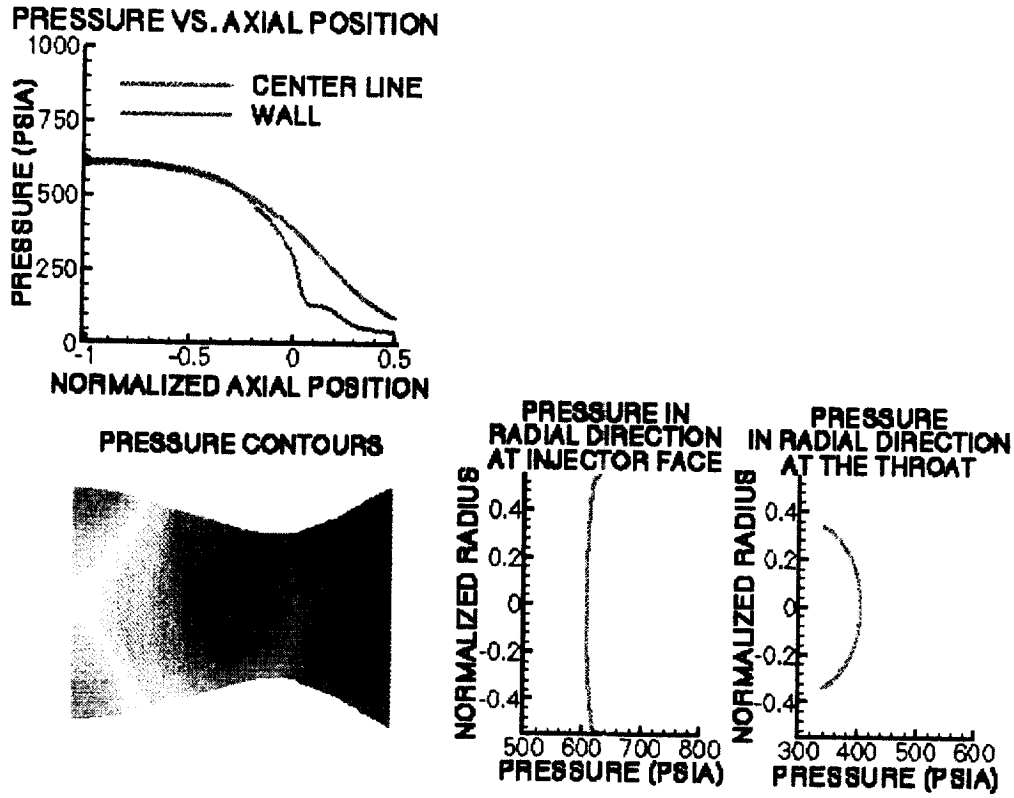

Figure 5a: Pressure pulse propagation in a combustion chamber in gaseous phase at a time interval.

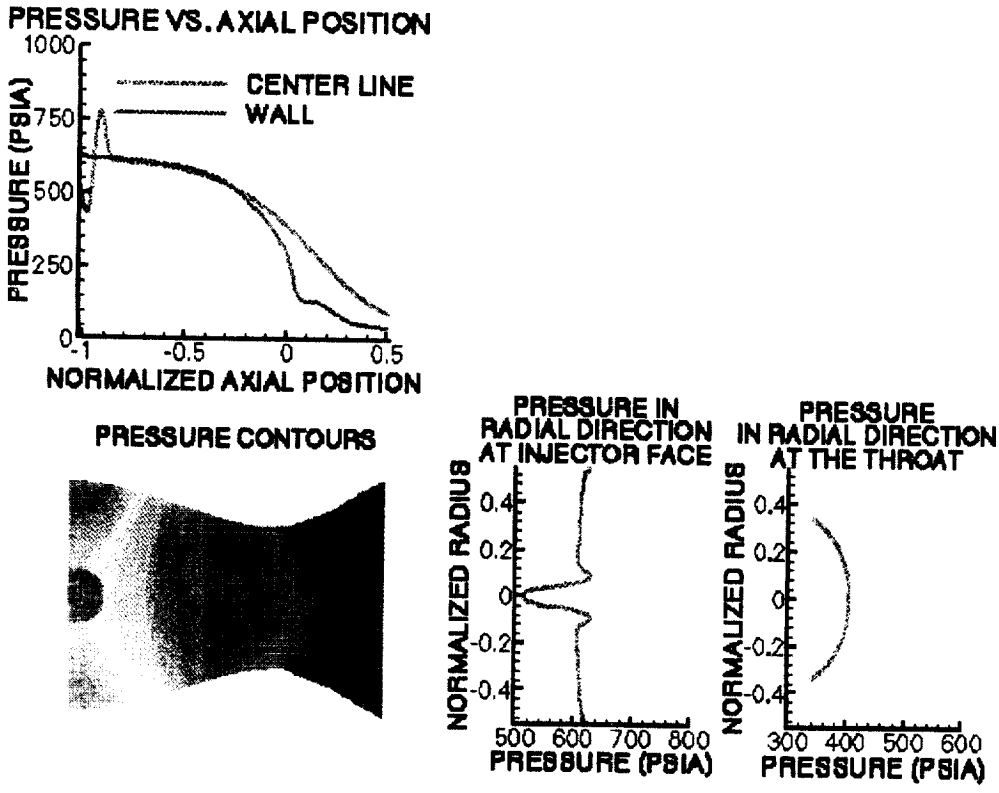

Figure 5b: Pressure pulse propagation in a combustion chamber in gaseous phase at a time interval.

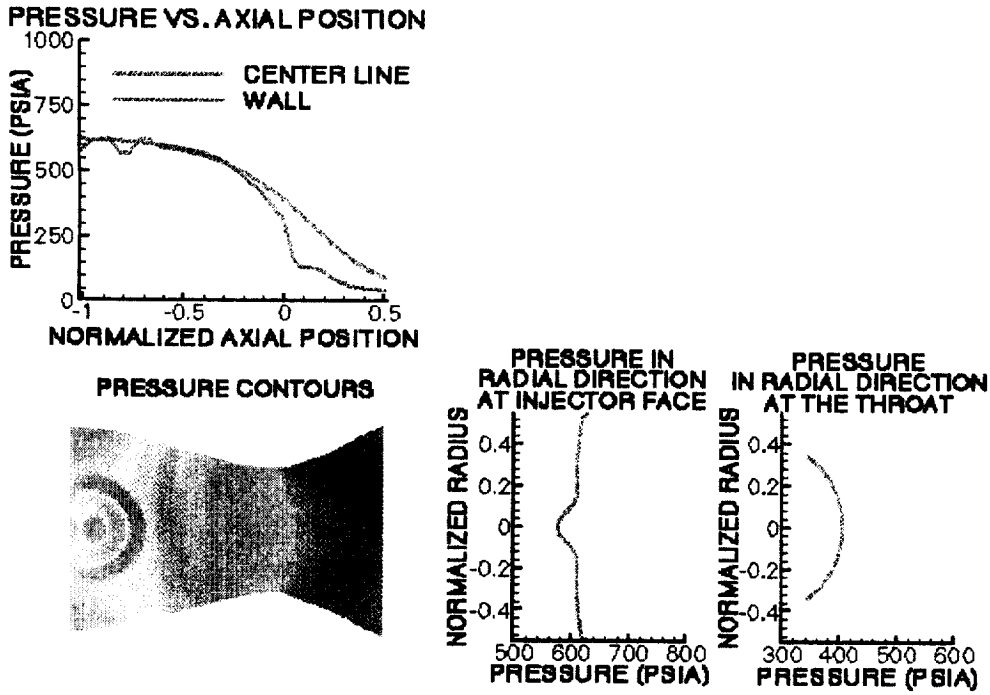

Figure 5c: Pressure pulse propagation in a combustion chamber in gaseous phase at a time interval.

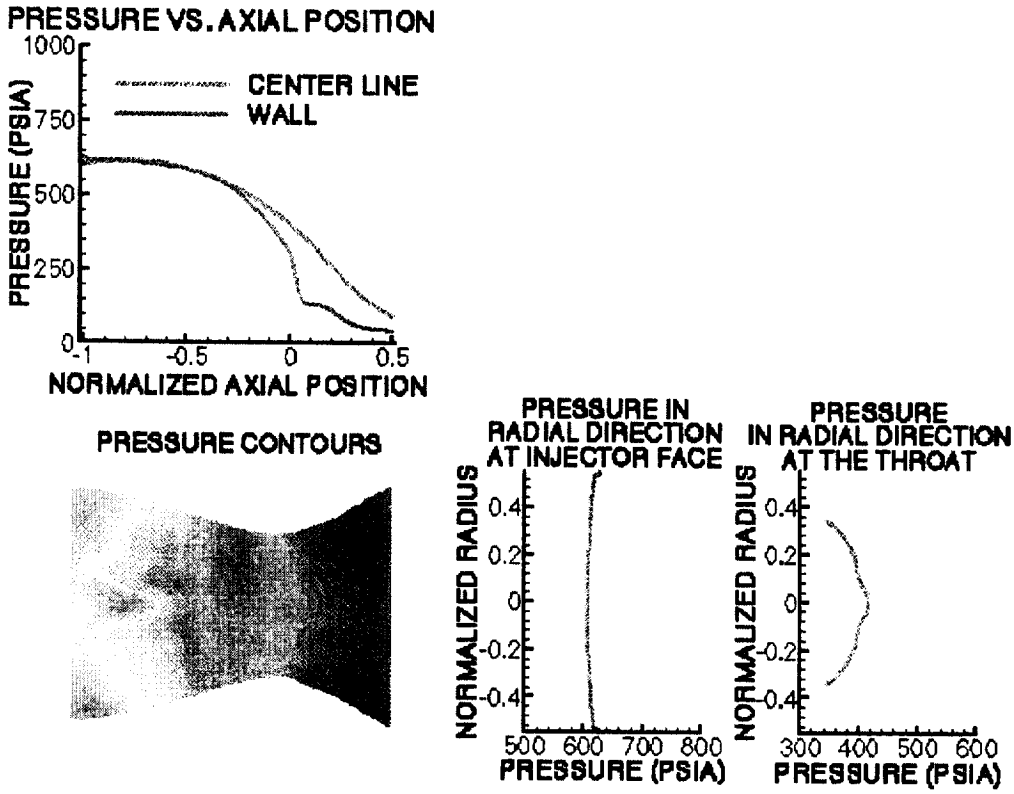

Figure 5d: Pressure pulse propagation in a combustion chamber in gaseous phase at a time interval.

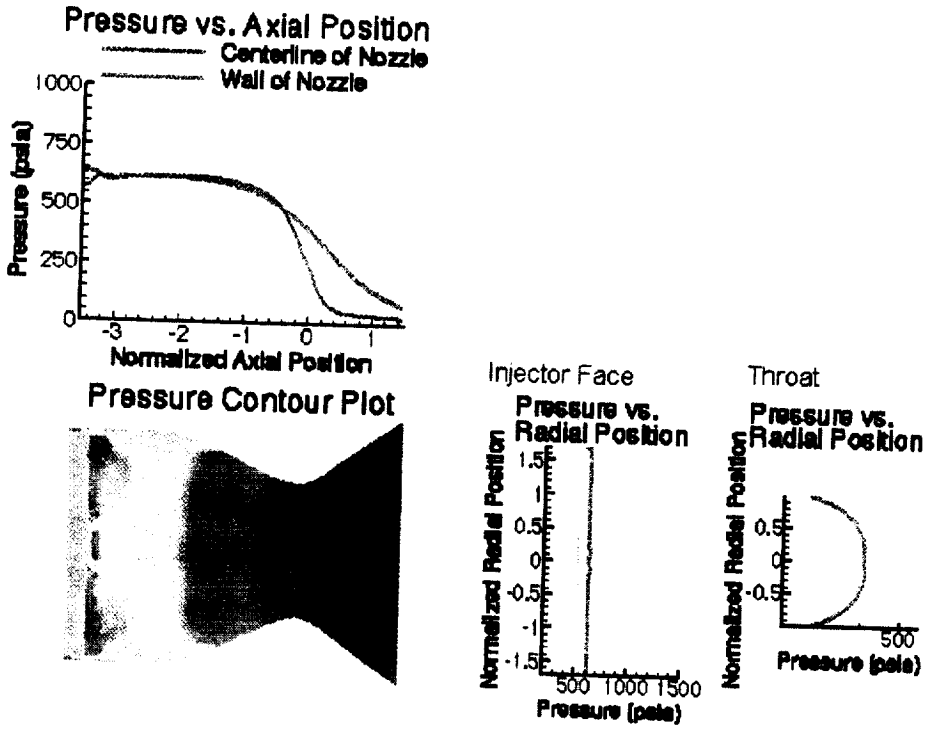

Figure 6a: Pressure pulse propagation in a combustion chamber in two phase flow at a time interval.

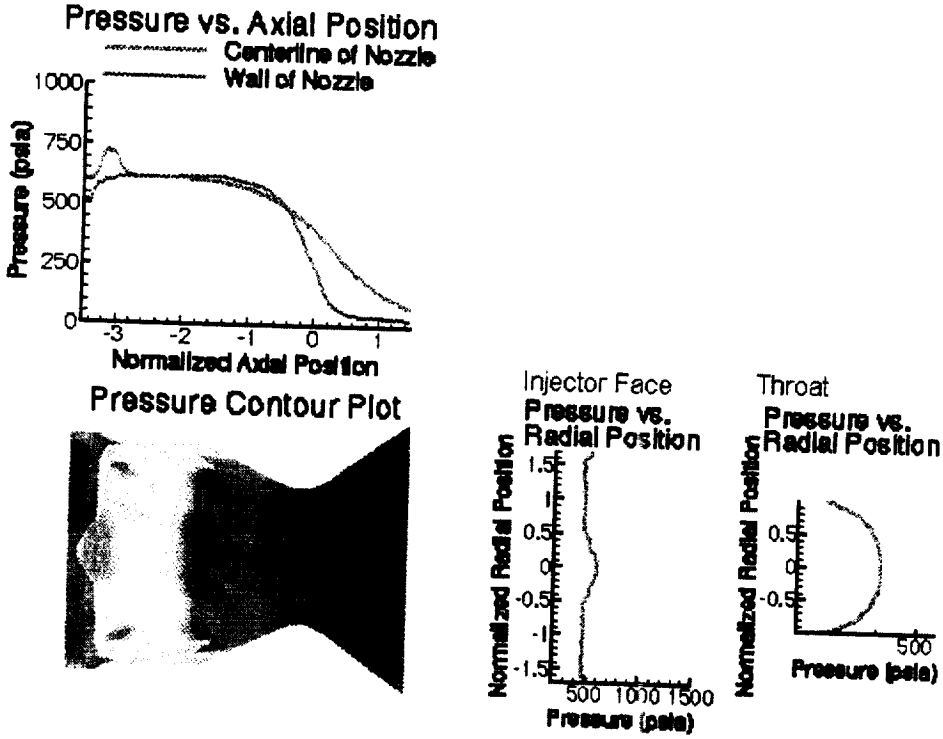

Figure 6b: Pressure pulse propagation in a combustion chamber in two phase flow at a time interval.

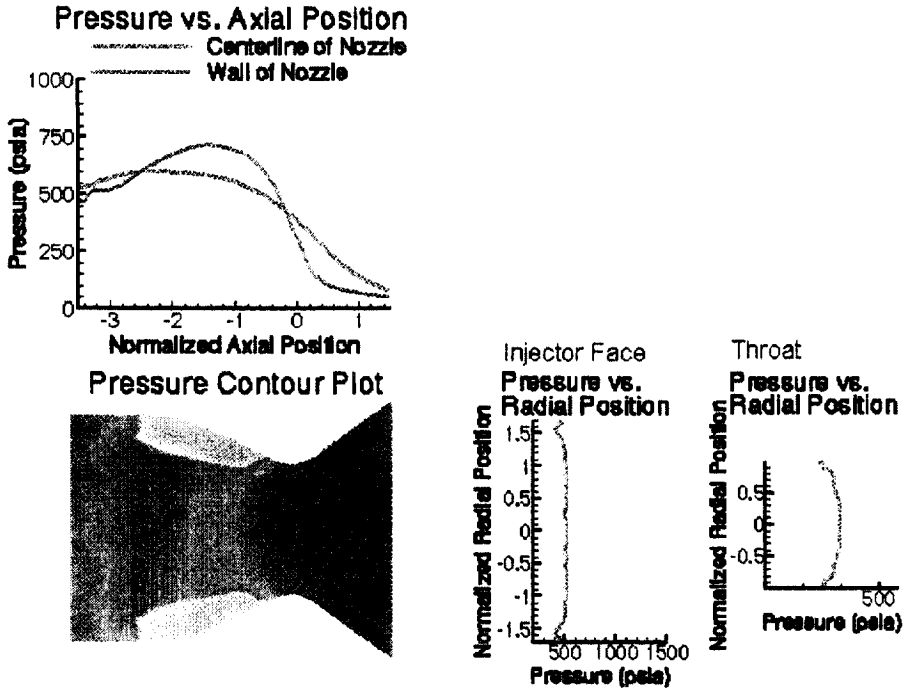

Figure 6c: Pressure pulse propagation in a combustion chamber in gaseous phase at a time interval.

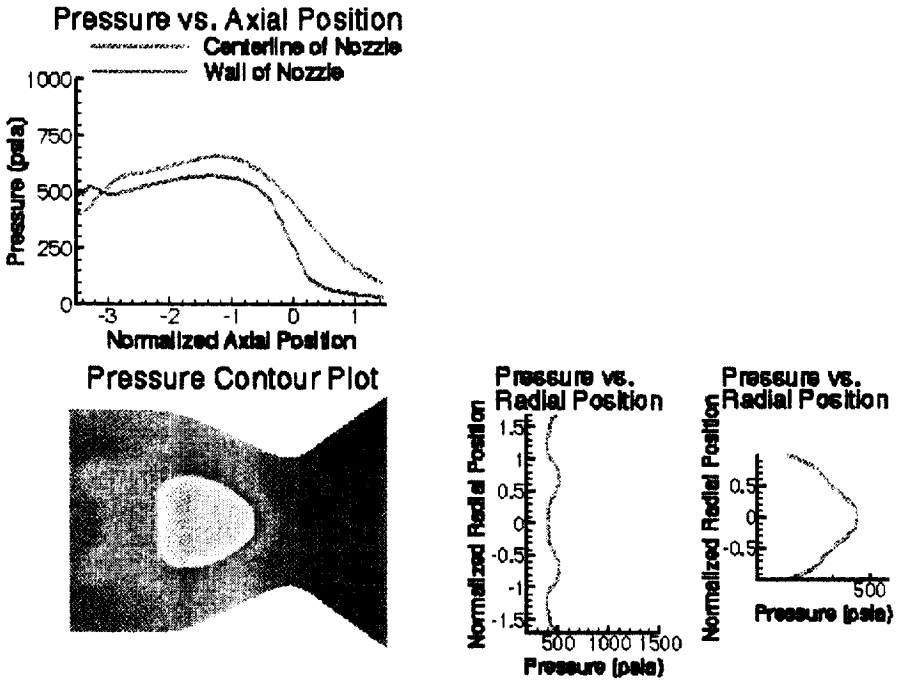

Figure 6d: Pressure pulse propagation in a combustion chamber in gaseous phase at a time interval.

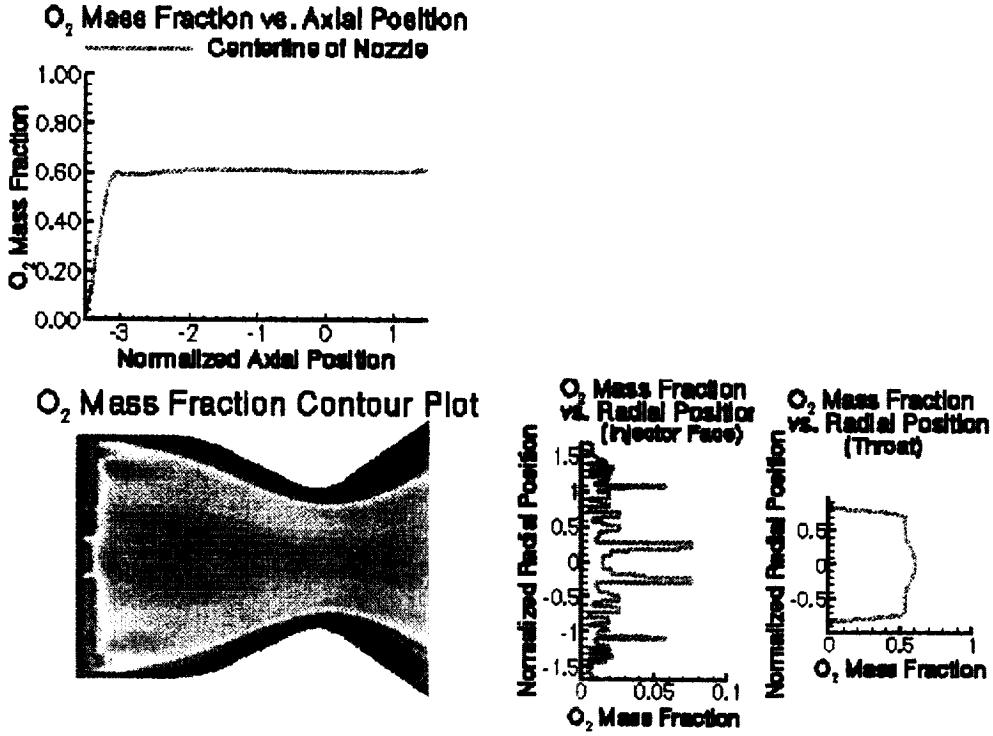

Figure 7a: O_2 Mass Fraction for two phase flow at steady state conditions.

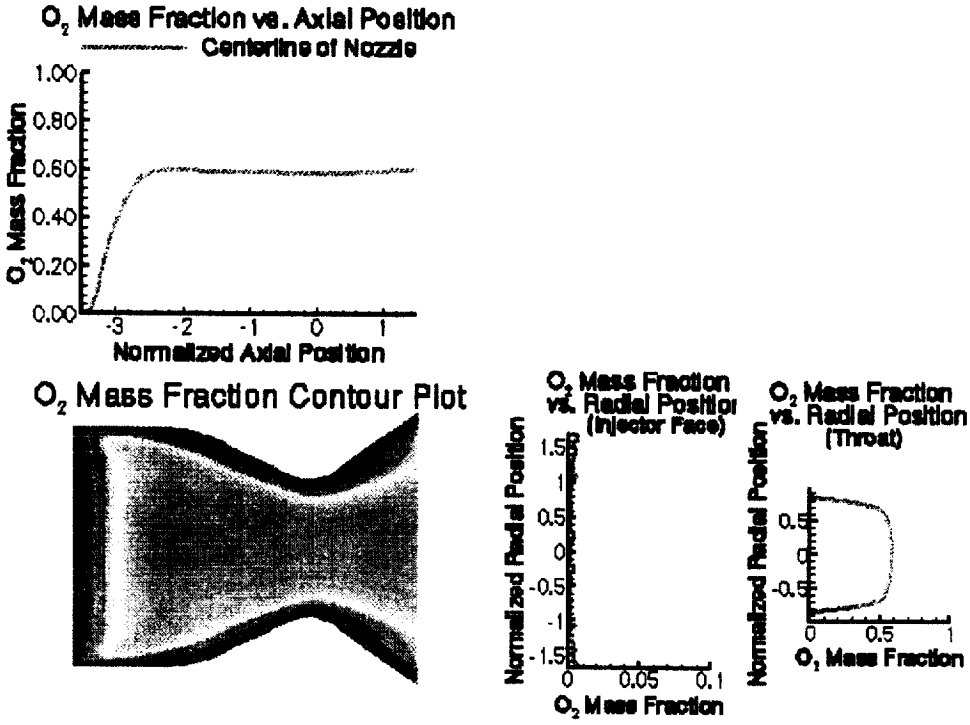

Figure 7b: O_2 Mass Fraction for two phase flow after the pressure pulse has been initiated.

Figure 8a: Schematic of a corrugated wall.

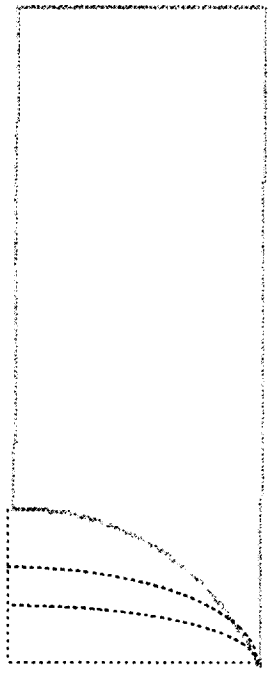

Figure 8b: Four variations of the lower wall, from circle to a flat plate.

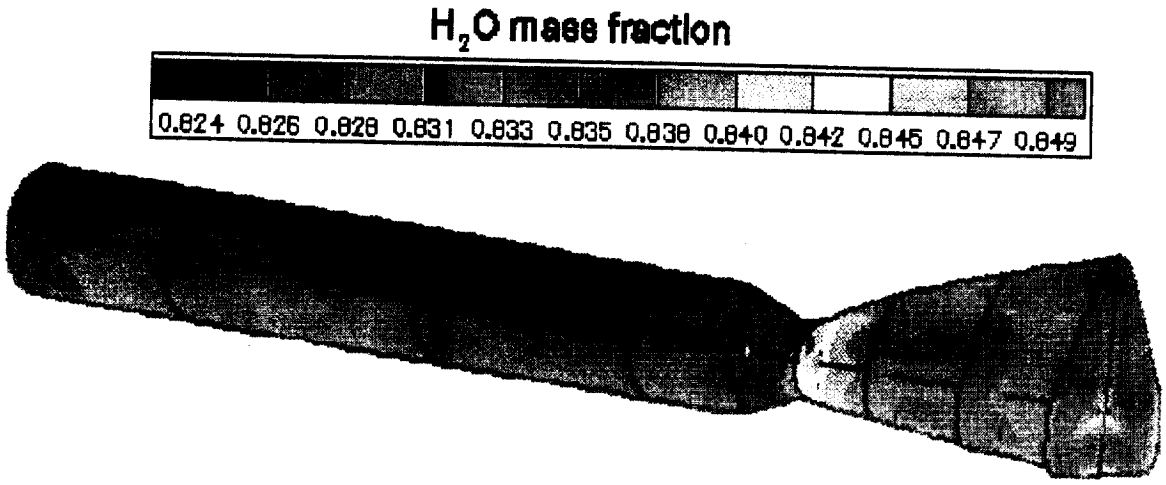

Figure 9d: Combined Cycle 3d analysis, contour plot of H_20 mass fraction.

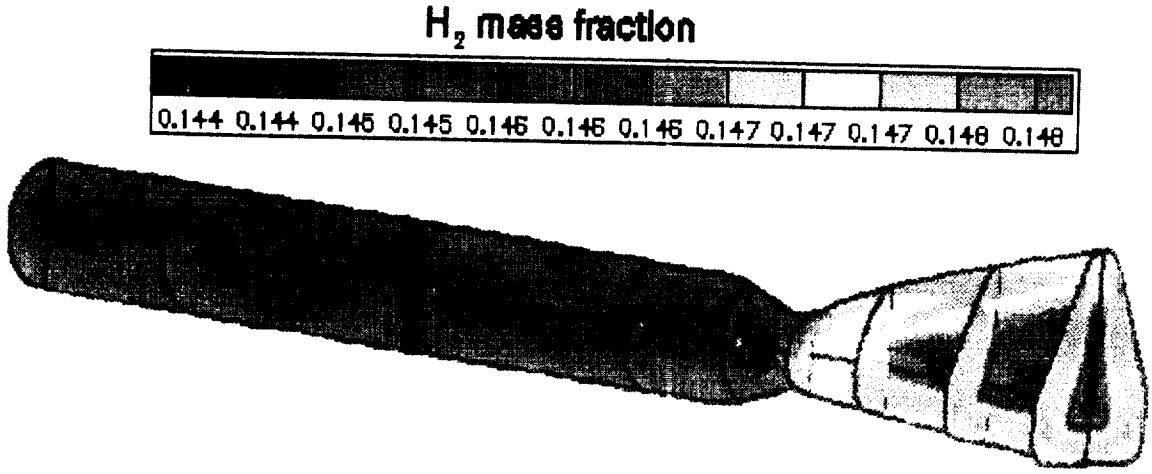

Figure 9e: Combined Cycle 3d analysis, contour plot of H_2 mass fraction.

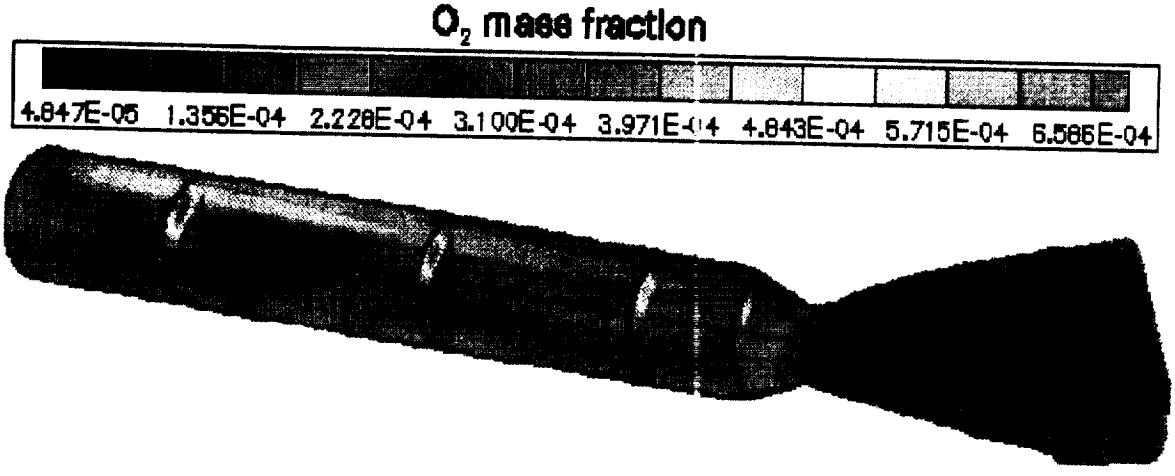

Figure 9f: Combined Cycle 3d analysis, contour plot of H_2 mass fraction.

Figure 9a: Combined Cycle 3d analysis, contour plot of mach number.

Figure 9b: Combined Cycle 3d analysis, contour plot of mach number along the plane of symmetry.

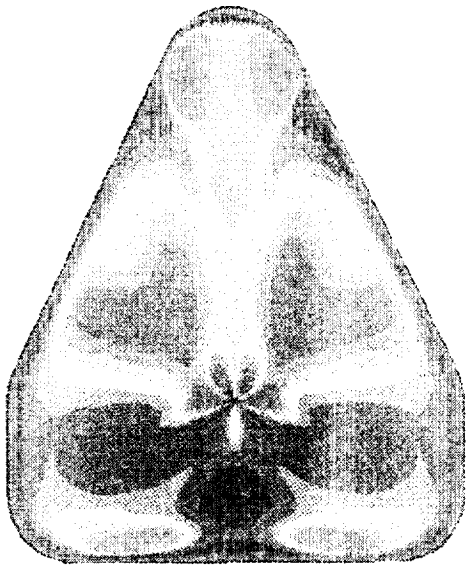

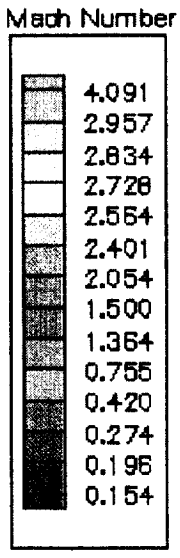

Figure 9c: Combined Cycle 3d analysis, contour plot of mach number along the exit plane